

Association of Glaucoma Risk Genes with Retinal Nerve Fiber Layer in a Multi-ethnic Asian Population: The Singapore Epidemiology of Eye Diseases Study

Xiaoran Chai,^{1,2,5} Kok Yao Low,^{1,3} Yih Chung Tham,¹ Miao Li Chee,¹ Sahil Thakur,¹ Liang Zhang,¹ Nicholas Y. Tan,¹ Chiea Chuen Khor,^{1,3,4} Tin Aung,^{1,3} Tien Yin Wong,^{1,3} and Ching-Yu Cheng¹⁻³

¹Singapore Eye Research Institute, Singapore National Eye Centre, Singapore

²Department of Ophthalmology, Yong Loo Lin School of Medicine, National University of Singapore, Singapore

³Ophthalmology & Visual Sciences Academic Clinical Program (Eye ACP), Duke-NUS Medical School, Singapore

⁴Genome Institute of Singapore, Agency for Science, Technology and Research, Singapore

⁵Biomedical Pioneering Innovation Center (BIOPIC), Beijing Advanced Innovation Center for Genomics (ICG), Peking University, Beijing, China

Correspondence: Ching-Yu Cheng, Singapore Eye Research Institute, The Academia, 20 College Road, Discovery Tower Level 6, Singapore 169856, Singapore; chingyu.cheng@duke-nus.edu.sg.

Received: March 4, 2020

Accepted: July 16, 2020

Published: August 21, 2020

Citation: Chai X, Low KY, Tham YC, et al. Association of glaucoma risk genes with retinal nerve fiber layer in a multi-ethnic asian population: The Singapore Epidemiology of Eye Diseases study. *Invest Ophthalmol Vis Sci.* 2020;61(10):37. <https://doi.org/10.1167/iovs.61.10.37>

PURPOSE. Genome-wide association studies have identified several genes associated with glaucoma. However, their roles in the pathogenesis of glaucoma remain unclear, particularly their effects on retinal nerve fiber layer (RNFL) thickness. The aim of this study was to investigate the associations between the identified glaucoma risk genes and RNFL thickness.

METHODS. A total of 3843 participants (7,020 healthy eyes) were enrolled from the Singapore Epidemiology of Eye Diseases (SEED) study, a population-based study composing of three major ethnic groups—Malay, Indian, and Chinese—in Singapore. Ocular examinations were performed, and spectral-domain optical coherence tomography (SD-OCT) was used to measure circumpapillary RNFL thickness. We selected 35 independent glaucoma-associated genetic loci for analysis. A linear regression model was conducted to determine the association of these variants with circumpapillary RNFL, assuming an additive genetic model. We conducted association analysis in each of the three ethnic groups, followed by a meta-analysis of them.

RESULTS. The mean age of the included participants was 59.4 ± 8.9 years, and the mean RNFL thickness is $92.3 \pm 11.2 \mu\text{m}$. In the meta-analyses, of the 35 glaucoma loci, we found that only *SIX6* was significantly associated with reduction in global RNFL thickness (rs33912345; $\beta = -1.116 \mu\text{m}$ per risk allele, $P = 1.64\text{E-}05$), and the effect size was larger in the inferior RNFL quadrant ($\beta = -2.015 \mu\text{m}$, $P = 2.9\text{E-}6$), and superior RNFL quadrant ($\beta = -1.646 \mu\text{m}$, $P = 6.54\text{E-}5$). The *SIX6* association were consistently observed across all three ethnic groups. Other than RNFL, we also found several genetic variants associated with vertical cup-to-disc ratio (*ATOH7*, *CDKN2B-AS1*, and *TGFBR3-CDC7*), rim area (*SIX6* and *CDKN2B-AS1*), and disc area (*SIX6*, *ATOH7*, and *TGFBR3-CDC7*). The association of *SIX6* rs33912345 with RNFL thickness remained similar after further adjusting for disc area and 3 other disc parameter associated SNPs (*ATOH7*, *CDKN2B-AS1*, and *TGFBR3-CDC7*).

CONCLUSIONS. Of the 35 glaucoma identified risk loci, only *SIX6* is significantly and independently associated with thinner RNFL. Our study further supports the involvement of *SIX6* with RNFL thickness and pathogenesis of glaucoma.

Keywords: glaucoma, RNFL, genetic diseases, Asian, meta-analysis

Glaucoma is one of the leading causes of blindness, affecting about 64 million people worldwide, and the number is projected to increase to 111.8 million by 2040.¹ It is a disease characterized by the progressive loss of retinal ganglion cells with structural changes to optic nerve, as well as retinal nerve fiber layers (RNFL). Of the various glaucoma subtypes, primary open angle glaucoma (POAG) is the most common form of glaucoma.¹

Understanding of the complex genetics underlying POAG has been aided by genome-wide association studies (GWAS), which identified several genes associated with the disease in the past decade.²⁻⁹ More recently, seven novel susceptibility loci were identified through a GWAS in Japan, highlighting the importance of ethnic difference in the development of the disease.¹⁰ Furthermore, GWAS meta-analyses also identified risk genes associated with glaucoma-related

endophenotypes, such as intraocular pressure (IOP) and optic disc parameters.^{2,8,11,12} Taking together, these studies contributed to a better understanding of the underlying genetics of glaucoma.

In addition to optic disc parameters, another important structural endophenotype of POAG is the circumpapillary RNFL thickness. Loss of RNFL may precede change in optic disc, in particular in early stages of glaucoma. RNFL thickness is a heritable trait,^{13,14} and *SIX6* and *CDKN2B-AS1* are the only loci consistently reported to be associated with reduction of RNFL thickness^{15–17}; moreover only a few studies have investigated the effect of glaucoma risk genes on RNFL thickness.^{17–19} Therefore the purpose of this study was to investigate the effects of known glaucoma risk variants on circumpapillary RNFL thickness.

METHODS

Study Population

Study subjects were enrolled from the Singapore Epidemiology of Eye Disease (SEED) Study, a population-based cohort comprising three major ethnic groups (Malays, Indians, and Chinese) in Singapore. The details of the study design and methodology of the SEED study were previously reported.^{20,21} In brief, the study was conducted in the southwestern part of Singapore, using a standardized study protocol. An age-stratified random sampling strategy was adopted in each ethnic group to select adults aged 40 or older. Optical coherence tomography (OCT) was performed at the the baseline examination of the Chinese participants (year 2009 to 2011), and at the six-year follow-up visit of the Malay (year 2011 to 2013), and Indian participants (year 2014 to 2016). The study adhered to the tenets of the Declaration of Helsinki, and ethics committee approval was obtained from the SingHealth Centralized Institutional Review Board. Institutional Review Board (IRB)/Ethics Committee approval was obtained for all participants.

Ocular Examination

All participants underwent a standardized and comprehensive ocular examination.^{21,22} In brief, IOP was measured using the Goldmann applanation tonometer (GAT; Haag-Streit, Bern, Switzerland) before pupil dilation. One reading was taken from each eye. If the IOP reading was greater than 21 mm Hg, a repeat reading was taken, and the second reading was used for analysis. Central corneal thickness (CCT) was measured using an ultrasound pachymeter (Advent; Mentor O & O, Inc., Norwell, MA, USA); the mean of five measurements was used for analysis. Axial length was measured using noncontact partial coherence interferometry (IOL Master V3.01; Carl Zeiss Meditec AG, Jena, Germany); the mean of five measurements was used for analysis.

Static automated perimetry (Swedish Interactive Threshold Algorithm standard 24-2, Humphrey Field Analyzer II; Carl Zeiss Meditec, Dublin, CA, USA) was performed on one in five participants and in all glaucoma subjects and glaucoma suspects (defined as below). A visual field was defined as reliable when fixation losses were less than 20%, and false-positive and false-negative rates were less than 33%. A glaucomatous visual field defect was defined as the presence of three or more significant ($P < 0.05$) non-edge contiguous points with at least one at the $P < 0.01$ level on the same side of the horizontal meridian in the pattern deviation

plot, and classified as “outside normal limits” on the Glaucoma Hemifield Test, confirmed on two consecutive visual field examinations. After pupil dilation using tropicamide 1% and phenylephrine hydrochloride 2.5%, the optic disc was evaluated using a 78-diopter (D) lens at 16 times magnification during slit-lamp funduscopy (Haag-Streit model BQ-900), and vertical cup-to-disc ration (VCDR) was measured with an eyepiece measuring graticule.

Spectral-Domain OCT Imaging

Optic nerve head (ONH) and circumpapillary RNFL imaging was performed using spectral-domain optical coherence tomography (SD-OCT; Cirrus HD-OCT; Carl Zeiss Meditec) after pupil dilation. Details of the Cirrus HD-OCT optic disc scan protocol have been described in detail elsewhere.²³ Briefly, optic nerve head and RNFL scan acquisitions were performed for each participant using an optic disc cube 200×200 scan protocol, which generated a cube of data in a 6×6 -mm² grid with 200×200 scans. The peripapillary measurement circle (3.46-mm diameter) was centered on the optic disc before capturing the image. After each capture, motion artifact was checked, and rescanning was performed if motion artifacts (indicated by discontinuity of blood vessels) or saccades through the peripapillary measurement circle were detected. The ONH and RNFL algorithms native to Cirrus HD-OCT (software version 6.0.2) were then used to measure the disc area, neural retinal rim area, and peripapillary RNFL thicknesses (average and quadrants) automatically. Detailed descriptions of the ONH and RNFL measurement algorithms have been previously published.²⁴ Study eyes with OCT scans showing retinal layer segmentation errors, signal strength of less than six, or artifacts due to eye movements or blinking were excluded from the analysis.

Definition of Glaucoma

In principle, glaucoma was defined according to the International Society of Geographical and Epidemiological Ophthalmology (ISGEO) criteria based on three categories.¹⁴ In brief, category 1 cases were defined as optic disc abnormality (VCDR or VCDR asymmetry ≥ 97.5 th percentile) with a corresponding glaucomatous visual field defect. Category 2 cases were defined as having a severely damaged optic disc (VCDR or VCDR asymmetry ≥ 99.5 th percentile) in the absence of reliable visual field test results. Category 3 cases were defined for subjects who were blind (corrected visual acuity $< 3/60$), without visual field or optic disc data, and previous glaucoma surgery or IOP > 99.5 th percentile.

A glaucoma suspect was defined as meeting any of the following criteria: (1) IOP > 21 mm Hg, (2) VCDR > 0.6 or VCDR asymmetry > 0.2 , (3) signs consistent with pseudoexfoliation or pigment dispersion syndrome, (4) narrow angles (posterior trabecular meshwork visible for $< 180^\circ$ during static gonioscopy), (5) peripheral anterior synechiae, (6) other findings consistent with secondary glaucoma, and (7) known history of glaucoma.

Genotyping

Genotyping was performed using the Illumina Infinium OmniExpress BeadChips (Illumina, Inc., San Diego, CA, USA). Stringent quality control filters were used to remove poorly performing samples and genetic variants.

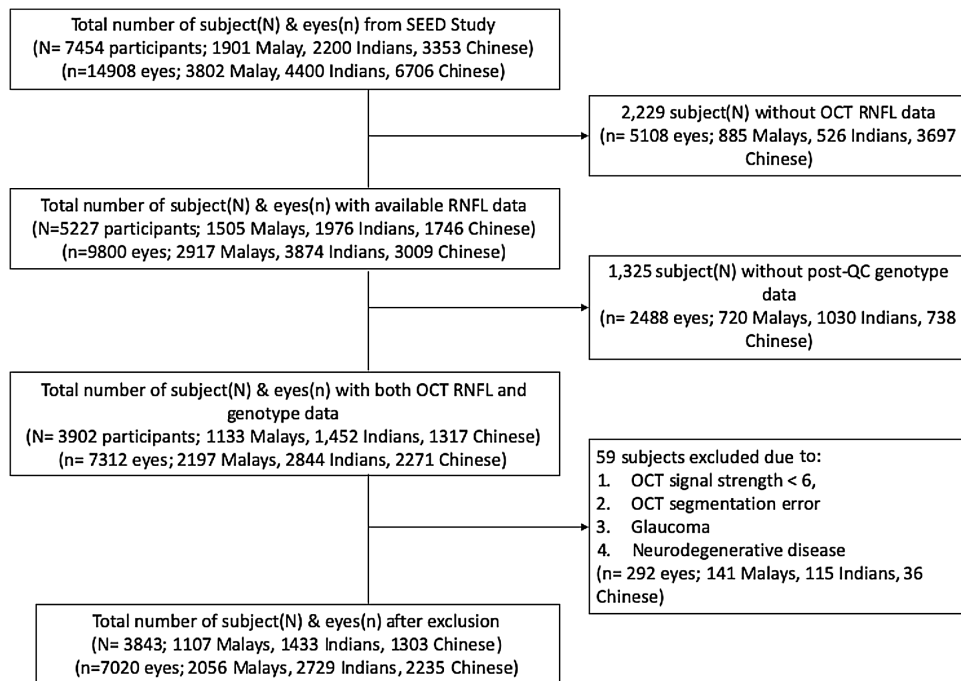


FIGURE. Consort diagram of study population.

with a call rate < 99%, minor allele frequency (MAF) < 0.1%, or showing deviation from Hardy-Weinberg equilibrium ($P < 10^{-6}$) were removed. Routine quality control criteria on a per sample basis were carried out, and poorly performing samples were removed from further analysis. The remaining samples were then subjected to biologic relationship verification by using the principle of variability in allele sharing according to the degree of relationship. Identity-by-state information was derived using the PLINK software.²⁵ For those pairs of individuals who showed evidence of cryptic relatedness, we removed the sample with the lower call rate before performing principal component (PC) analysis. Principal component analysis was undertaken using EIGENSTRAT²⁶ to account for spurious associations resulting from ancestral differences of individual SNPs.

We conducted an extensive literature review on published GWAS of POAG and identified loci reported to be genome-wide significant ($P < 5 \times 10^{-8}$) to date.^{2,4-10,16,27-31} We identified a total of 52 genetic variants from 35 POAG genetic loci (Supplementary Table S1).

Statistical Analysis

A linear regression model was fitted to determine the association between the the risk alleles and RNFL thickness, as well as VCDR, rim area and disc area. We assumed an additive genetic model where the genotype of the genetic variant was a variable varying from 0, 1, or 2, representing the number of copies of the risk allele carried. We conducted association analysis in each ethnic group, followed by a meta-analysis combining all three ethnic groups. Analysis for the association was adjusted for age, sex, and the first three PCs in each ethnic groups.

Data from two eyes of the individuals were included in the analysis when data from both eyes were available. If one eye was excluded or not eligible, data from the other eye

were used. Generalized estimating equations with exchangeable correlation structures were applied to account for the correlation between pairs of eyes for each individual. In the meta-analysis, significance level of per-variant analysis was defined as $P < 0.0014$ after Bonferroni correction (0.05/35 for testing 35 loci). We performed conditional analysis to assess the independent association of *SIX6* SNPs with RNFL thickness. Here we used nominal $P < 0.05$ as the significance cutoff instead of the one corrected for multiple testing because only one association test was performed for *SIX6* SNP rs33912345. All association analyses were done using R package “geepack.”

RESULTS

Of the 7454 SEED subjects who participants in the ocular examination, 5227 had available OCT RNFL data. We further excluded 1325 individuals without post-quality control genotype, and 59 with major ocular diseases or unacceptable RNFL data. This left a total of 7020 healthy eyes from 3843 participants (1303 Chinese, 1433 Indians, and 1107 Malays) with OCT, clinical and demographic data for this analysis (Fig.). The clinical and demographic characteristics of the study subjects are shown in Table 1. The mean (standard deviation [SD]) age was 55.0 (7.3) years for Chinese, 61.5 (8.4) years for Indians, and 61.8 (9.2) years for Malays in our study. The overall mean (SD) RNFL thickness in the study was 92.3 (11.2) μm .

In the single cohort analysis, *SIX6* single nucleotide polymorphisms (SNP) rs33912345 was significantly associated with superior RNFL in Chinese individuals ($\beta = -2.479$, $P = 0.001$) (Supplementary Table S3), but not significantly associated with global RNFL and inferior RNFL in all 3 populations (Supplementary Tables S2, S4). In addition, the risk allele of *ABCA1* SNP (rs2472494) was significantly associated

TABLE 1. Demographic and Clinical Characteristic of the Study Subjects

Characteristics	Overall	Chinese	Indian	Malay	P Value*
Number of subjects	3843	1303	1433	1107	
Number of Eyes	7020	2235	2729	2056	
Age, yr	59.4 (8.9)	55.0 (7.3)	61.5 (8.4)	61.8 (9.2)	<0.001
Gender, female	1928 (50.2)	644 (49.4)	711 (49.6)	573 (51.8)	0.452
Intraocular pressure, mm Hg	14.8 (3.0)	14.3 (3.0)	15.3 (2.8)	14.5 (3.0)	<0.001
Vertical cup-to-disc ratio	0.5 (0.1)	0.5 (0.1)	0.6 (0.1)	0.5 (0.1)	< 0.001
Disc area, mm ²	2.0 (0.4)	2.0 (0.4)	2.0 (0.4)	2.1 (0.4)	< 0.001
RNFL thickness, μm					
Global	92.3 (11.2)	96.5 (9.6)	87.1 (10.6)	94.6 (10.8)	< 0.001
Temporal sector	65.5 (12.8)	71.7 (12.2)	58.8 (10.9)	67.8 (11.4)	< 0.001
Superior sector	115.4 (17.7)	121.3 (16.6)	108.6 (16.4)	118.0 (17.5)	< 0.001
Nasal sector	69.3 (11.0)	68.1 (10.7)	69.2 (11.0)	70.8 (11.0)	< 0.001
Inferior sector	118.8 (18.4)	124.6 (16.8)	111.9 (17.2)	121.8 (18.6)	< 0.001

Data are presented as mean (standard deviation) or number (%), as appropriate by eye.

TABLE 2. Associations of Lead SNPs With RNFL Thickness Parameters From Combined Analyses of All Three Ethnic Groups

Gene	rs ID	Risk Allele	Global RNFL		Superior Quadrant		Inferior Quadrant	
			β*	P Value	β*	P Value	β*	P Value
<i>8q22</i>	rs284489	A	0.454	0.045	0.693	0.056	0.799	0.036
<i>ABCA1</i>	rs2472494	T	-0.127	0.574	-0.070	0.847	-0.523	0.169
<i>AFAP1</i>	rs4619890	G	-0.194	0.401	-0.533	0.141	-0.232	0.556
<i>ANKH</i>	rs76325372	C	0.205	0.410	0.225	0.568	0.272	0.510
<i>ANKRD55</i>	rs61275591	A	-0.229	0.418	-0.177	0.698	-0.091	0.850
<i>ARHGEF12</i>	11:120357425	AT/A	-0.468	0.061	-0.331	0.400	-0.919	0.031
<i>ATOH7</i>	rs1900004	T	-0.202	0.427	0.471	0.252	-0.367	0.395
<i>ATXN2</i>	rs7137828	C	-0.128	0.877	0.277	0.826	-0.721	0.607
<i>CADM2</i>	rs34201102	G	0.445	0.072	0.516	0.185	0.581	0.158
<i>CAV1/2</i>	rs10281637	C	-0.349	0.446	-0.199	0.772	-0.521	0.481
<i>CDKN1A</i>	6:36592986	TCA/T	-0.540	0.039	-0.472	0.254	-0.922	0.042
<i>CDKN2B-AS1</i>	rs1360589	T	-0.749	0.019	-0.979	0.052	-1.269	0.015
<i>DGKG</i>	rs9853115	T	0.132	0.573	0.308	0.409	0.327	0.400
<i>EXOC2</i>	rs2073006	T	-0.627	0.057	-0.651	0.213	-1.178	0.033
<i>FLNB</i>	rs12494328	A	0.018	0.935	-0.092	0.798	-0.298	0.425
<i>FMNL2</i>	rs56117902	C	0.241	0.457	0.087	0.861	0.276	0.602
<i>FNDC3B</i>	rs7636836	T	-0.557	0.350	-1.680	0.110	-0.813	0.460
<i>FOXC1</i>	rs2745572	A	-0.090	0.720	-0.163	0.680	-0.224	0.597
<i>GAS7</i>	rs9913991	A	-0.365	0.409	-0.408	0.583	-1.135	0.129
<i>GMDS</i>	rs11969985	G	-0.128	0.679	-0.076	0.880	-0.190	0.713
<i>HMGA2</i>	rs343093	G	-0.128	0.597	-0.165	0.665	-0.392	0.333
<i>IKZF2</i>	rs56335522	C	0.301	0.756	1.021	0.492	1.455	0.355
<i>LHPP</i>	rs12262706	G	-0.314	0.214	-0.680	0.094	-0.590	0.167
<i>LMO7</i>	rs9530458	T	-0.181	0.570	-0.204	0.675	-0.212	0.685
<i>LMX1B</i>	rs10819187	G	0.207	0.447	0.142	0.738	0.173	0.707
<i>LOXL1</i>	rs1048661	T	0.158	0.489	0.077	0.834	0.152	0.693
<i>MEIS2</i>	rs28480457	C	0.402	0.424	-0.103	0.899	-0.065	0.940
<i>PDE7B</i>	rs9494457	A	0.155	0.505	0.366	0.313	0.176	0.644
<i>PMM2</i>	rs3785176	G	0.475	0.094	0.891	0.043	0.679	0.155
<i>SIX6</i>	rs33912345	C	-1.116	1.64E-5	-1.646	6.54E-5	-2.015	2.9E-6
<i>TAP2</i>	rs241430	C	0.153	0.478	0.056	0.873	0.421	0.246
<i>TGFBR3-CDC7</i>	rs1192415	G	-0.048	0.865	-0.033	0.939	0.099	0.830
<i>TMCO1</i>	rs4656461	G	-1.362	0.026	-1.873	0.052	-1.122	0.285
<i>TMTC2</i>	rs324794	G	-0.117	0.686	-0.103	0.821	-0.301	0.531
<i>TXNRD2</i>	rs35934224	T	0.650	0.107	0.869	0.148	1.065	0.108

In bold, Bonferroni-corrected significance value $P < 0.0014$ (0.05/35).

*β, Changes in RNFL thickness (in micrometers) per risk allele count. Model adjusted for age, gender, top three genotype PCs.

with thinner inferior RNFL thickness in Malays ($\beta = -2.378$ μm per risk allele, $P = 0.001$; Supplementary Table S4).

Table 2 shows the association of the glaucoma loci with RNFL thickness in the meta-analysis of all three ethnic

groups. The lead variant within a locus, defined by the variant with the most significant P value from the meta analysis of global RNFL, was reported. Of the 35 loci included in the analysis, only *SIX6* SNP (rs33912345) was significantly

TABLE 3. Association of SNPs With Vertical Cup-to-Disc Ratio, Rim Area, and Disc Area From Combined Analyses of Three Ethnic Groups

Gene	rs ID	Risk Allele	Vertical Cup-to-Disc Ratio		Rim Area, Mm ²		Disc Area, Mm ²	
			β^*	P Value	β^*	P Value	β^*	P Value
<i>8q22</i>	rs284489	A	0.002	0.451	0.003	0.529	0.012	0.182
<i>ABCA1</i>	rs2472494	T	0.004	0.211	-0.010	0.069	-0.002	0.797
<i>AFAP1</i>	rs4619890	G	-0.003	0.313	0.001	0.896	-0.012	0.168
<i>ANKH</i>	rs76325372	C	-0.005	0.125	0.012	0.041	0.003	0.769
<i>ANKRD55</i>	rs61275591	A	0.009	0.032	-0.017	0.014	0.005	0.652
<i>ARHGEF12</i>	11:120357425	AT/A	0.006	0.096	-0.012	0.041	-0.001	0.912
<i>ATOH7</i>	rs1900004	T	-0.018	1.29E-6	-0.015	0.014	-0.087	<1E-8
<i>ATXN2</i>	rs7137828	C	-0.003	0.812	0.002	0.918	-0.011	0.718
<i>CADM2</i>	rs34201102	G	-0.001	0.806	-0.002	0.781	-0.006	0.499
<i>CAV1/2</i>	rs10281637	C	0.002	0.733	-0.004	0.691	0.002	0.900
<i>CDKN1A</i>	6:36592986	TCA/T	0.005	0.133	-0.020	0.002	-0.008	0.420
<i>CDKN2B-AS1</i>	rs1360589	T	0.016	1.42E-4	-0.026	3.87E-4	0.010	0.405
<i>DGKG</i>	rs9853115	T	0.006	0.072	-0.005	0.415	0.003	0.762
<i>EXOC2</i>	rs2073006	T	0.007	0.088	-0.012	0.126	-0.003	0.798
<i>FLNB</i>	rs12494328	A	0.007	0.027	-0.014	0.011	0.001	0.953
<i>FMNL2</i>	rs56117902	C	0.003	0.473	-0.006	0.438	0.007	0.552
<i>FNDC3B</i>	rs7636836	T	0.005	0.554	-0.018	0.237	-0.007	0.792
<i>FOXC1</i>	rs2745572	A	0.005	0.114	-0.005	0.387	0.008	0.397
<i>GAS7</i>	rs9913991	A	-0.004	0.557	0.000	0.974	-0.019	0.304
<i>GMDS</i>	rs11969985	G	0.006	0.167	-0.013	0.073	-0.002	0.896
<i>HMGA2</i>	rs343093	G	0.002	0.454	-0.011	0.047	-0.011	0.248
<i>IKZF2</i>	rs56335522	C	0.007	0.571	-0.027	0.200	-0.039	0.292
<i>LHPP</i>	rs12262706	G	0.000	0.980	-0.009	0.170	-0.011	0.257
<i>LMO7</i>	rs9530458	T	0.001	0.813	-0.006	0.409	-0.004	0.742
<i>LMX1B</i>	rs10819187	G	0.001	0.892	0.004	0.541	0.006	0.606
<i>LOXL1</i>	rs1048661	T	0.002	0.542	-0.007	0.221	-0.001	0.936
<i>MEIS2</i>	rs28480457	C	-0.004	0.520	-0.006	0.591	-0.031	0.112
<i>PDE7B</i>	rs9494457	A	-0.004	0.182	0.007	0.225	-0.001	0.950
<i>PMM2</i>	rs3785176	G	0.002	0.529	-0.001	0.825	0.008	0.470
<i>SIX6</i>	rs33912345	C	0.010	0.006	-0.052	<1E-8	-0.055	3.42E-8
<i>TAP2</i>	rs241430	C	0.000	0.900	0.001	0.913	0.002	0.844
<i>TGFBR3-CDC7</i>	rs1192415	G	0.014	2.08E-4	0.012	0.078	0.072	<1E-8
<i>TMCO1</i>	rs4656461	G	0.014	0.095	-0.030	0.034	0.003	0.905
<i>TMTC2</i>	rs324794	G	-0.003	0.380	-0.007	0.298	-0.024	0.028
<i>TXNRD2</i>	rs35934224	T	-0.013	0.012	0.025	0.007	-0.001	0.919

In bold, Bonferroni-corrected significance value $P < 0.0014$ (0.05/35).

* β denotes per unit changes in respective outcome parameter, per risk allele count. Model adjusted for age, gender, top three genotype PCs.

associated with global ($P = 1.64E-05$), superior ($P = 6.54E-05$) and inferior ($P = 2.9E-06$) RNFL thickness. The effect size of rs33912345 was largest in the inferior RNFL ($\beta = -2.015$) followed by the superior ($\beta = -1.646$) and global RNFL quadrant ($\beta = -1.116$). Other seven loci reached nominal significant level ($P < 0.05$), including *CDKN1A*, *CDKN2B-AS1* and *8q22* in the global and inferior RNFL thickness, *TMCO1* in the global RNFL thickness, *ARHGEF12*, *EXOC2* in the inferior RNFL thickness, and *PMM2* in the superior RNFL thickness.

In addition to RNFL thickness, we also conducted association tests for other glaucoma endophenotypes including VCDR, rim area, and disc area to check whether the same set of genetic variants are responsible for the change in these glaucoma-related structure phenotypes. *SIX6* was significantly associated with both rim area ($\beta = -0.052$, $P < 1E-8$) and disc area ($\beta = -0.055$, $P = 3.42E-8$), but not VCDR ($P = 0.006$). *CDKN2B-AS1* was associated with both VCDR ($\beta = 0.016$, $P = 1.42E-4$) and rim area ($\beta = -0.026$, $P = 3.87E-4$), but not disc area ($P = 0.405$). *ATOH7* was asso-

ciated with both VCDR ($\beta = -0.018$, $P = 1.29E-6$) and disc area ($\beta = -0.087$, $P < 1E-8$), but not rim area ($P = 0.014$). And *TGFBR3-CDC7* was associated with VCDR ($\beta = 0.014$, $P = 2.08E-4$) only (Table 3).

Because *SIX6* is associated with several glaucoma endophenotypes (RNFL, rim area and disc area), we further included disc area as one of the covariates when testing the association between *SIX6* and RNFL thickness. After adjusting for disc area, *SIX6* was still significantly associated with global RNFL ($\beta = -0.882$, $P = 4.9E-4$), superior RNFL ($\beta = -1.2162$, $P = 2.6E-3$), and inferior RNFL ($\beta = -1.7115$, $P = 5.7E-5$) (Table 4) in the meta-analysis of three populations. In addition, after further adjusting for *ATOH7* rs1900004, *CDKN2B-AS1* rs1360589, and *TGFBR3-CDC7* rs1192415, the effect size and significance level still remained similar (Table 4) in the meta-analysis of three populations. These sensitivity analyses suggest that *SIX6* SNP is independently associated with RNFL thickness.

On the other hand, for *ATOH7* rs1900004 and *TGFBR3-CDC7* rs1192415, after further adjusting for disc area, the

TABLE 4. Association Between *SIX6* (rs33912345) and Peripapillary Retinal Nerve Fiber Thickness Parameters From Combined Analyses of Three Ethnic Groups

	Global RNFL		Superior Quadrant		Inferior Quadrant	
	β^*	<i>P</i> Value	β^*	<i>P</i> Value	β^*	<i>P</i> Value
Model 1 [†]	-0.882	4.9E-4	-1.216	2.6E-3	-1.712	5.7E-5
Model 2 [‡]	-0.847	8.8E-4	-1.172	4.0E-3	-1.682	8.4E-5

* Changes in RNFL thickness (in μm) per risk allele C of rs33912345.

[†] Model 1 adjusted for age, gender, top three genotype PCs, and disc area.

[‡] Model 2 adjusted for age, gender, top three genotype PCs, disc area, rs1900004 (*ATOH7* gene), rs1360589 (*CDKN2B-AS1*), rs1192415 (*TGFB3-CDC7*).

associations with VCDR became non-significant (data not shown), suggesting that the original observed associations with VCDR of the two genes were mainly driven by their associations with disc area, also given the known correlation between disc area and VCDR.

We also conducted two more sensitivity analyses for all the variants by including axial length and disc area as additional covariates in the original model (Supplementary Tables S5, S6, respectively). The associations between all variants (including *SIX6*) and RNFL remained similar in these sensitivity analyses.

DISCUSSION

Of the 35 known POAG risk loci included in our study, we found that only *SIX6* rs33912345 was significantly associated with thinner RNFL in normal healthy eyes. The association was more apparent in the superior and inferior quadrant, consistent with previous reports.^{18,32} In our study, we also noticed that the association between *SIX6* and RNFL remains similar after further adjusting for disc area and the other three disc parameters associated SNPs suggesting that this association is independent of disc size as well as other disc related genotypes. Our findings provided a more comprehensive insight into the complex genetic architecture underlying glaucoma and the role of *SIX6* in determining RNFL thinning. This suggests that subjects with the *SIX6* genetic risk variant are at higher risk for glaucoma due to thinner RNFL, while the other glaucoma risk genes may lead to glaucoma through mechanisms.

The human *SIX* gene consists of *SIX1-SIX6*, was initially discovered through homology to *Drosophila melanogaster* (*Drosophila*) *sine oculis* (*so*) gene, and its function is important for ectodermal differentiation and ocular development.³³ Carnes et al.³² first reported their association with RNFL thinning and hypothesized that *SIX6* causes glaucoma by disrupting neural retinal tissue development leading to loss of retinal ganglion cells eventually leading to glaucomatous visual loss. The association of *SIX6* with thinning of RNFL was later confirmed by several other studies.^{17,18,34,35} These associations were also found to apply to nonglaucomatous eyes by one of our earlier studies with smaller sample size of 1243 Chinese individuals,¹⁶ which strongly supported *SIX6*'s contribution to RNFL thickness.¹⁶ In the article, each copy of C allele of rs33912345 was associated with 1.44- μm decrease in global RNFL thickness. Similarly, Kuo et al.¹⁷ reported the association between RNFL thickness and another SNP rs10483727 in a population of 231 individuals of European descent; each T allele of rs10483727 was associated with 0.16 μm decrease in global RNFL thickness. Khawaja et al.³⁴ have also reported

association of rs33912345 C allele with smaller rim area (0.030-mm decrease, $P = 5.4\text{E-}9$), a larger VCDR (0.025 increase, $P = 3.3\text{E-}10$) and thinner RNFL (0.39- μm decrease, $P = 0.001$). This is also an European based study. They used 3699 samples to estimate the association between the *SIX6* SNP and RNFL, and 5433 samples to estimate the associations between the *SIX6* SNP and rim/VCDR parameters. As such, our finding of association of *SIX6* with thinner RNFL further reinforces these previous findings in a larger cohort.

The risk allele of *SIX6* (rs33912345) was associated with thinner global RNFL ($\beta = -1.116$, $P = 2.9\text{E-}6$ per risk allele) in our analysis, and was previously reported to be associated with higher POAG risk.³⁶ In addition, *CDKN1A*, *CDKN2B-AS1*, *8q22*, *TMCO1*, *ARHGEF12*, *EXOC2*, *PMM2* were associated with thinner RNFL thickness parameters (either global, inferior, or superior) but with nominal significance ($P < 0.05$). Of these seven loci, the risk alleles of *CDKN1A*, *CDKN2B-AS1*, *TMCO1*, *ARHGEF12*, *EXOC2* were also associated with increased risk of POAG, based on previous reports.³⁷⁻³⁹ On the other hand, the risk allele of *8q22* (rs284489), was previously reported to be associated with normal tension glaucoma⁴⁰ but was shown to be associated with thicker global RNFL ($\beta = 0.454$, $P = 0.045$) in our meta-analysis. Similarly, the risk allele of *PMM2* (rs3785176) was previously reported to be associated with higher POAG risk⁴¹ but was shown to be associated with thicker superior RNFL ($\beta = 0.891$, $P = 0.043$) in our current analysis. Nevertheless, it should be noted that the associations RNFL thickness in these two loci were only marginally significant. Thus further investigation is needed to further confirm whether a differing direction with RNFL and glaucoma risk was indeed present in these two loci.

Based on Tables 2 and 3, we observed that the risk allele of *SIX6* was significantly associated with thinner RNFL thickness ($P = 1.64\text{E-}5$), and consistently showed to be associated with smaller rim area ($P = 1\text{E-}8$). In addition, its association with vertical cup-to-disc ratio (VCDR) was nominally significant ($P = 0.006$) but with consistent direction (per risk allele, larger VCDR). The less significant association with VCDR may be partly owing to the reason that thinning of RNFL and rim area are better proxy markers for RGC compared to VCDR. Furthermore, it should be noted that *SIX6* was also significantly associated with smaller disc area ($P = 3.42\text{E-}8$). In light of this and given that VCDR is an indirect measure of rim loss that is calculated from the cup length (which can also be thought of as "disc length minus the rim length") and disc length—it is therefore possible that the association with VCDR was slightly negated compared to associations with rim area and disc area.

Other than *SIX6*, of the 35 loci only one of the other previously identified POAG risk genes, *ABCA1*, were

significantly associated with reduction in inferior RNFL thickness in our Malay group, despite that there loci (including *ATOH7*, *CDKN2B-AS* and *TGFBR3-CDC7* SNPs) are significantly associated with glaucoma-related disc parameters. We therefore postulated that glaucoma risk genes may have different effects on RNFL thinning and disc alteration, and RNFL thinning in glaucoma is most likely a manifestation of various ocular insults rather than a direct effect of the gene products and their associated pathway on the integrity of RNFL. Further studies are needed to evaluate the mechanisms in which these genes predispose individuals to glaucoma.

The strength of our study includes a multiethnic population-based sample with a standardized protocol for RNFL assessment. Nevertheless, our study has a few limitations. First, our study is limited by its cross-sectional design, and thus we cannot determine whether individuals carrying the *SIX6* risk variants have an accelerated rate of RNFL thinning, or that the risk variants only have an effect during the embryological ocular development phase which results in these individuals having a thinner RNFL. A prospective study might be useful to distinguish between these mechanisms via which the variant may have effect. On the other hand, based on our power calculation, given a type 1 error rate of 0.0014, the current sample size of 7020 would have 80% power to minimally detect an effect size of 1.01 μm in RNFL thickness per risk allele (for allele frequency of 0.2), and 0.78 μm per risk allele (for allele frequency of 0.4). Thus our current sample size may be limited in identifying new loci especially one with lower allele frequency.

In conclusion, this is the first study comparing effect of glaucoma risk genes on RNFL across multiple ethnic groups in Asians. Of the 35 glaucoma risk loci we investigated in our population, only *SIX6* is significantly and independently associated with thinner RNFL in the global, superior and inferior RNFL quadrants. Our study further supports the involvement of *SIX6* with RNFL thickness and pathogenesis of glaucoma. These findings may provide further insights into the genetic variants associated with pathogenesis of glaucoma.

Acknowledgments

Supported by the National Medical Research Council (NMRC/1249/2010, NMRC/CIRG/1371/2013, NMRC/CIRG/1417/2015, and NMRC/CIRG/1488/2018), Singapore. C-YC is supported by National Medical Research Council (NMRC/CSA-SI/0012/2017).

Disclosure: **X. Chai**, None; **K.Y. Low**, None; **Y.C. Tham**, None; **M.L. Chee**, None; **S. Thakur**, None; **L. Zhang**, None; **N.Y. Tan**, None; **C.C. Khor**, None; **T. Aung**, None; **T.Y. Wong**, None; **C.-Y. Cheng**, None

References

1. Tham Y-C, Li X, Wong TY, et al. Global prevalence of glaucoma and projections of glaucoma burden through 2040: a systematic review and meta-analysis. *Ophthalmology*. 2014;121:2081–2090.
2. Nakano M, Ikeda Y, Tokuda Y, et al. Common variants in *CDKN2B-AS1* associated with optic-nerve vulnerability of glaucoma identified by genome-wide association studies in Japanese. *PLoS One*. 2012;7:e33389.
3. Ramdas WD, van Koolwijk LM, Lemij HG, et al. Common genetic variants associated with open-angle glaucoma. *Hum Mol Genet*. 2011;20:2464–2471.
4. Osman W, Low S-K, Takahashi A, et al. A genome-wide association study in the Japanese population confirms 9p21 and 14q23 as susceptibility loci for primary open angle glaucoma. *Hum Mol Genet*. 2012;21:2836–2842.
5. Thorleifsson G, Walters GB, Hewitt AW, et al. Common variants near *CAV1* and *CAV2* are associated with primary open-angle glaucoma. *Nat Genet*. 2010;42:906–909.
6. Burdon KP, Macgregor S, Hewitt AW, et al. Genome-wide association study identifies susceptibility loci for open angle glaucoma at *TMCO1* and *CDKN2B-AS1*. *Nat Genet*. 2011;43:574–578.
7. Chen Y, Lin Y, Vithana EN, et al. Common variants near *ABCA1* and in *PMM2* are associated with primary open-angle glaucoma. *Nat Genet*. 2014;46:1115–1119.
8. Springelkamp H, Iglesias AI, Mishra A, et al. New insights into the genetics of primary open-angle glaucoma based on meta-analyses of intraocular pressure and optic disc characteristics. *Hum Mol Genet*. 2017;26:438–453.
9. Choquet H, Paylakhi S, Kneeland SC, et al. A multiethnic genome-wide association study of primary open-angle glaucoma identifies novel risk loci. *Nat Commun*. 2018;9:2278.
10. Shiga Y, Akiyama M, Nishiguchi KM, et al. Genome-wide association study identifies seven novel susceptibility loci for primary open-angle glaucoma. *Hum Mol Genet*. 2018;27:1486–1496.
11. Hysi PG, Cheng C-Y, Springelkamp H, et al. Genome-wide analysis of multi-ancestry cohorts identifies new loci influencing intraocular pressure and susceptibility to glaucoma. *Nat Genet*. 2014;46:1126–1130.
12. Wiggs JL, Yaspan BL, Hauser MA, et al. Common variants at 9p21 and 8q22 are associated with increased susceptibility to optic nerve degeneration in glaucoma. *PLoS Genet*. 2012;8:e1002654.
13. van Koolwijk LM, Despriet DD, van Duijn CM, et al. Genetic contributions to glaucoma: heritability of intraocular pressure, retinal nerve fiber layer thickness, and optic disc morphology. *Invest Ophthalmol Vis Sci*. 2007;48:3669–3676.
14. Hougaard JL, Kessel L, Sander B, et al. Evaluation of heredity as a determinant of retinal nerve fiber layer thickness as measured by optical coherence tomography. *Invest Ophthalmol Vis Sci*. 2003;44:3011–3016.
15. Yoshikawa M, Nakanishi H, Yamashiro K, et al. Association of glaucoma-susceptible genes to regional circumpapillary retinal nerve fiber layer thickness and visual field defects. *Invest Ophthalmol Vis Sci*. 2017;58:2510–2519.
16. Cheng C-Y, Allingham RR, Aung T, et al. Association of common *SIX6* polymorphisms with peripapillary retinal nerve fiber layer thickness: the Singapore Chinese Eye Study Association of *SIX6* Variant With RNFL Thickness. *Invest Ophthalmol Vis Sci*. 2015;56:478–483.
17. Kuo JZ, Zangwill LM, Medeiros FA, et al. Quantitative trait locus analysis of *SIX1-SIX6* with retinal nerve fiber layer thickness in individuals of European descent. *Am J Ophthalmol*. 2015;160:123–130.e1.
18. Cheng C-Y, Allingham RR, Aung T, et al. Association of common *SIX6* polymorphisms with peripapillary retinal nerve fiber layer thickness: the Singapore Chinese Eye Study. *Invest Ophthalmol Vis Sci* 2015;56:478–483.
19. Mydel P, Wang Z, Brisslert M, et al. Carbamylation-dependent activation of T cells: a novel mechanism in the pathogenesis of autoimmune arthritis. *J Immunol*. 2010;184:6882–6890.
20. Foong AW, Saw S-M, Loo J-L, et al. Rationale and methodology for a population-based study of eye diseases in Malay people: The Singapore Malay Eye Study (SiMES). *Ophthalmic Epidemiol*. 2007;14:25–35.
21. Lavanya R, Jeganathan VSE, Zheng Y, et al. Methodology of the Singapore Indian Chinese Cohort (SICC) eye study:

- quantifying ethnic variations in the epidemiology of eye diseases in Asians. *Ophthalmic Epidemiol.* 2009;16:325–336.
22. Chua J, Tham YC, Liao J, et al. Ethnic differences of intraocular pressure and central corneal thickness: the Singapore Epidemiology of Eye Diseases study. *Ophthalmology.* 2014;121:2013–2022.
 23. Cheung CY, Chen D, Wong TY, et al. Determinants of quantitative optic nerve measurements using spectral domain optical coherence tomography in a population-based sample of non-glaucomatous subjects. *Invest Ophthalmol Vis Sci.* 2011;52:9629–9635.
 24. Tham Y-C, Cheung CY, Koh VT, et al. Relationship between ganglion cell-inner plexiform layer and optic disc/retinal nerve fibre layer parameters in non-glaucomatous eyes. *Br J Ophthalmol.* 2013;97:1592–1597.
 25. Purcell S, Neale B, Todd-Brown K, et al. PLINK: a tool set for whole-genome association and population-based linkage analyses. *Am J Hum Genet.* 2007;81:559–575.
 26. Price AL, Patterson NJ, Plenge RM, et al. Principal components analysis corrects for stratification in genome-wide association studies. *Nat Genet.* 2006;38:904–909.
 27. Gharahkhani P, Burdon KP, Fogarty R, et al. Common variants near ABCA1, AFAP1 and GMDS confer risk of primary open-angle glaucoma. *Nat Genet.* 2014;46:1120–1125.
 28. Bailey JNC, Loomis SJ, Kang JH, et al. Genome-wide association analysis identifies TXNRD2, ATXN2 and FOXC1 as susceptibility loci for primary open-angle glaucoma. *Nat Genet.* 2016;48:189–194.
 29. Gharahkhani P, Burdon KP, Bailey JNC, et al. Analysis combining correlated glaucoma traits identifies five new risk loci for open-angle glaucoma. *Sci Rep.* 2018;8:3124.
 30. Shiga Y, Akiyama M, Nishiguchi KM, et al. Genome-wide association study identifies seven novel susceptibility loci for primary open-angle glaucoma. *Hum Mol Genet.* 2018;27:1486–1496.
 31. Micheal S, Ayub H, Khan MI, et al. Association of known common genetic variants with primary open angle, primary angle closure, and pseudoexfoliation glaucoma in Pakistani cohorts. *Mol Vis.* 2014;20:1471–1479.
 32. Carnes MU, Liu YP, Allingham RR, et al. Discovery and functional annotation of SIX6 variants in primary open-angle glaucoma. *PLoS Genet.* 2014;10:e1004372.
 33. Kumar J. The sine oculis homeobox (SIX) family of transcription factors as regulators of development and disease. *Cell Mol Life Sci.* 2009;66:565–583.
 34. Khawaja AP, Chan MP, Yip JL, et al. A common glaucoma-risk variant of SIX6 alters retinal nerve fiber layer and optic disc measures in a European population: the EPIC-Norfolk Eye Study. *J Glaucoma.* 2018;27:743–749.
 35. Shiga Y, Nishiguchi KM, Kawai Y, et al. Genetic analysis of Japanese primary open-angle glaucoma patients and clinical characterization of risk alleles near CDKN2B-AS1, SIX6 and GAS7. *PLoS One.* 2017;12:e0186678.
 36. Bailey JN, Loomis SJ, Kang JH, et al. Genome-wide association analysis identifies TXNRD2, ATXN2 and FOXC1 as susceptibility loci for primary open-angle glaucoma. *Nat Genet.* 2016;48:189–194.
 37. Springelkamp H, Iglesias AI, Mishra A, et al. New insights into the genetics of primary open-angle glaucoma based on meta-analyses of intraocular pressure and optic disc characteristics. *Hum Mol Genet.* 2017;26:438–453.
 38. Gharahkhani P, Burdon KP, Fogarty R, et al. Common variants near ABCA1, AFAP1 and GMDS confer risk of primary open-angle glaucoma. *Nat Genet.* 2014;46:1120–1125.
 39. MacGregor S, Ong JS, An J, et al. Genome-wide association study of intraocular pressure uncovers new pathways to glaucoma. *Nat Genet.* 2018;50:1067–1071.
 40. Nordberg A, Hartvig P, Lilja A, et al. Decreased uptake and binding of 11C-nicotine in brain of Alzheimer patients as visualized by positron emission tomography. *J Neural Transm Park Dis Dement Sect.* 1990;2:215–224.
 41. Chen Y, Lin Y, Vithana EN, et al. Common variants near ABCA1 and in PMM2 are associated with primary open-angle glaucoma. *Nat Genet.* 2014;46:1115–1119.